Available online at www.sciencedirect.com
SCIENCE DIRECT
Polymer 47 (2006) 3874–3888
polymer
www.elsevier.com/locate/polymer

Morphology and mechanical properties of polyamide 12/polypropylene blends in presence and absence of reactive compatibiliser

S. Jose [a], B. Francis [a], S. Thomas [a,*], J. Karger-Kocsis [b]

[a] School of Chemical Sciences, Mahatma Gandhi University, Priyadarshini Hills P.O., Kottayam 686 560, Kerala, India
[b] Institut für Verbundwerkstoffe GmbH (Institute for Composite Materials), Kaiserslautern University of Technology, P.O. Box 3049, D-67653 Kaiserslautern, Germany

Received 16 November 2005; received in revised form 12 February 2006; accepted 13 March 2006
Available online 18 April 2006

Abstract

Blends of polyamide 12 (PA12) and isotactic polypropylene (PP) were prepared by melt mixing in an internal mixer in presence and absence of compatibilisers. The compatibiliser used was maleic anhydride functionalised polypropylene (PP-*g*-MA). Effect of compatibilisation on the blends has been evaluated from the morphological parameters derived from scanning electron micrographs (SEM) of cryogenically fractured and extracted surfaces of the specimens. The uncompatibilised blends showed two-phase unstable morphology due to high interfacial tension and coalescence effects in the absence of favourable interactions at interface between the individual phases. Incompatibility increased as the concentration of dispersed phase in the blend increased. Compatibilisation stabilised the morphology by reducing the particle size as well as interparticle distance and enhancing the interfacial area and interface adhesion. A critical concentration of compatibiliser required for effective compatibilisation (CMC) was observed beyond which there was no net improvement in interfacial properties and was considered as the point of interfacial saturation. Experimental results were compared with the compatibilisation theories of Noolandi and Hong and Leibler and based on the calculated average interfacial area occupied per compatibiliser molecule it was concluded that the molecular state of compatibiliser at interface changed with concentration. It was supported by the rate constant for change in interfacial tension (K) values which experienced a maximum at CMC followed by drastic reduction. Mechanical properties of the uncompatibilised blends showed inferior properties. It was found that compatibilisation significantly improved the mechanical properties. A good correlation has been observed between the mechanical properties and morphological parameters.

Keywords: Morphology; Interfacial tension; Reactive compatibilisation

1. Introduction

It is widely recognised that the morphology is the principal deciding factor of ultimate properties of a heterogeneous polymer blend system. The blend morphology is determined by factors which are related to material parameters and processing conditions. A major complicating factor in the case of immiscible polymer blends is the intrinsic instability of the morphology in the melt, which depends on shear or elongational stress, viscosity ratio, blend composition, interfacial tension and processing temperature. Usually, immiscible polymer blends are characterised by a coarse and unstable morphology coupled with poor interfacial adhesion between the individual phases. Therefore, the real problem ought to have been paying attention in the field of multiphase polymer blend systems is the manipulation of the phase structure via judicious control of the melt flow during processing and the interfacial interactions.

The fundamental reasons responsible for the unstable morphology are the unfavourable interactions at the interface between the components which create a high-interfacial energy and low interfacial thickness, which would, in turn lead to poor interfacial adhesion between the phases that may result in premature failure of the interface upon stress transfer. Another aspect that deserves attention is the coalescence of the dispersed phase, which makes the dispersed particles larger and non-uniform, leading to an unstable morphology. Therefore, the key to overcome problems related to the coarse morphology of multi component polymer blends is to (a) reduce the interfacial tension in the melt, (b) diminish the rate of coalescence under static and quiescent conditions

* Corresponding author. Tel.: +91 481 2730003; fax: +91 481 2731002.
E-mail addresses: sabut552001@yahoo.com (S. Thomas), sabut@sancharnet.in (S. Thomas).

0032-3861/$ - see front matter © 2006 Elsevier Ltd. All rights reserved.
doi:10.1016/j.polymer.2006.03.046

and (c) improve the interfacial adhesion between the phases in the solid state. These can be achieved in presence of compatibilisers, which are interfacial agents that can stabilise the immiscible polymer blends, just like surfactants or detergents in oil–water emulsions.

Compatibilisation of multiphase polymer systems has been reviewed extensively in literature [1–3]. It is well established that compatibilisation can be achieved either by addition of pre synthesised copolymer (physical compatibilisation) or through the in situ generation of graft or block copolymers at the interface between the individual polymers by chemical reactions during processing (reactive compatibilisation). Several researchers have employed physical compatibilisation strategy in heterogeneous blend systems and found that presence of copolymers at the interface drastically decreased the dispersed particle size and thereby improved the morphological stability [4–10]. However, in this case, one should take care of the fact that the copolymer stays at the interface without dissolving in either of the two polymers and/or forming a mesophase of micelle structure. Further, it should also be taken into account that the stable location of the copolymer at the interface essentially depends on the composition, molecular weight and the molecular architecture of the copolymer as well as its miscibility with the individual phases [11–15]. Very recently, Kim et al. [16] demonstrated that compatibilisation of an immiscible blend can be achieved by the addition of a gradient copolymer during melt processing.

In recent years, more attention has been focused on reactive compatibilisation technique as it is very fast, easy and cost effective alternative. The basic principle underlying reactive compatibilisation is that one can generate graft or block copolymers in situ by making use of the functionalities present in one or more polymers, during melt processing. These in situ formed copolymers act as compatibilisers by reducing interfacial tension and coalescence rate and improving interfacial adhesion. This method has been employed in a number of blend systems [17–41] especially those containing polyamide (PA) as one of the components due to its inherent chemical functionalities, i.e. amine or carboxyl groups and even amide linkage itself. Effect of reactive compatibilisation on the morphology of polymer blends has been reported several times in literature [19–23]. Very recently, Zhang et al. [24] examined the interfacial morphology development during the processing of polystyrene/poly methyl methacrylate (PS/PMMA) by reactive coupling. These authors, using atomic force microscopy (AFM) and transmission electron microscopy (TEM) have demonstrated that the coupling reaction at the initial stage is rapid and interfacial roughness (emulsification) is obtained even at 5 min of annealing. In the light of these studies, it can be concluded that refining and stabilizing effects of a compatibiliser on blend morphology depend on its ability to lower the interfacial tension [25–27] and to decrease the possibility of coalescence of droplets [25,26,28] which, in turn, depend on several factors such as the type and amount of the functional group present in compatibiliser [28–34], reactive group content and end group configuration of the polymer [35,36], the miscibility of the compatibiliser with one of the phases [28] and its conformation, molecular architecture and stability at the interface [37–41].

The present research work aims at making fundamental investigations on the effect of reactive compatibilisation on the morphology and mechanical properties of PA12/polypropylene (PP) blends. PA12 exhibits excellent mechanical (including impact) and thermal properties, but is expensive, while PP is one of the cheapest and lightest commodity thermoplastics with good strength and solvent resistance but poor impact properties. Blending these two polymers would lead to a new cost effective polymeric material with good mechanical and thermal properties coupled with excellent solvent resistance. However, these blends are highly immiscible and incompatible owing to the unfavourable interfacial interactions. In the present work, PP grafted with maleic anhydride (PP-*g*-MA) was used as the compatibiliser which can improve the compatibility of the blends through interfacial chemical reactions. The main objective of the present study is to monitor the effect of compatibilisation on morphological parameters such as size, distribution (pdi), interfacial area per unit volume (A_i) and inter particle distance (IPD) of dispersed droplets. Attempts have also been made to compare the experimental results with the established compatibilisation theories. Further, the mechanical properties are correlated with the morphology of the blends in presence and absence of compatibiliser.

2. Experimental

2.1. Materials

Isotactic PP (Koylene 3060) having a melt flow index (MFI) of 3 dg/min (at 230 °C/2.16 kg) and a density of 0.90 g/cm^3 was kindly supplied by Indian Petro Chemicals Limited, Baroda, Gujarat, India. PA12, (Vestamid, L1670) having a melt volume-flow rate (MVR) of 60 cm^3/10 min (at 250 °C/2.16 kg) and a density of 1.01 g/cm^3 was kindly supplied by Degussa, High Performance Polymers, Marl, Germany. PP-*g*-MA (Polybond 3200) having MFI 110 dg/min and MA content 1.0 wt% was obtained by the courtesy of Crompton Corporation, Middlebury, USA.

2.2. Preparation of uncompatibilised and compatibilised PA12/iPP blends

Both compatibilised and uncompatibilised blends were prepared by melt mixing process in a Brabender Plastograph. Appropriate amounts of PA12 and PP were mixed at 185 °C and 60 rpm for 6 min to obtain blends of different compositions (PA12/PP = 90/10, 80/20, 70/30, 60/40, 50/50, 40/60, 30/70, 20/80 and 10/90). These blends are represented as N_{90}, N_{80} and so on where subscripts represent the weight percent of PA12. Blends containing 30, 50 and 70 wt% of PP (N_{70}, N_{50} and N_{30}, respectively) were selected for compatibilisation. Compatibilised blends were obtained in two-step mixing process. In the first step, the compatibiliser was premixed with PP for 2 min at 185 °C and 60 rpm and in the second step PA12 was added to

this mixture and mixing was continued further for 6 min. The amount of compatibiliser was varied from 1 to 20 wt% (in the case of N_{70} up to 15 wt%) to determine the optimum compatibiliser concentration. Both uncompatibilised and compatibilised blends were compression moulded to obtain sheets of 2 mm thickness for mechanical testing.

2.3. Morphology of blends

The specimens for morphology studies were cryogenically fractured in liquid nitrogen. In PP rich blends, the dispersed PA phase was etched with formic acid at ambient temperature for 48 h. In PA rich blends boiling xylene was used (for 72 h) to extract the PP dispersed phase preferentially. The extracted surface was sputter coated by gold for 150 s. A minimum of five photographs was taken for each sample using a scanning electron microscope (SEM; Jeol 5400, Tokyo, Japan). About 200 particles were considered to determine the droplet diameter of the dispersed phase using image analysis software. The number ($\bar{D}_n$) and weight ($\bar{D}_w$) average diameters were determined using the following equations.

The number average diameter:

$$\bar{D}_n = \frac{\sum Ni\bar{D}i}{\sum Ni} \tag{1}$$

The weight average diameter:

$$\bar{D}_w = \frac{\sum Ni\bar{D}i^2}{\sum Ni\bar{D}i} \tag{2}$$

From the dispersed droplet type morphology, morphological parameters such as polydispersity index (pdi), interfacial are per unit volume (A_i) [21] and interparticle distance (IPD) [42] were calculated using the following expressions

$$\text{pdi} = \frac{\bar{D}_w}{\bar{D}_n} \tag{3}$$

$$A_i = \frac{3\phi}{R} \tag{4}$$

$$\text{IPDC} = D\left[\left(\frac{\pi}{6\phi}\right)^{1/3} - 1\right] \tag{5}$$

where ϕ is the volume fraction of the dispersed phase and D and R the number average diameter and radius of the dispersed particles, respectively.

2.4. Tensile properties of blends

Tensile specimens were punched out from the compression-moulded sheets. The specimens were dried for 3 h in a vacuum oven prior to the tensile test. Tensile tests were performed in accordance with ASTM D412-80 test method using dumb-bell shaped test pieces at a crosshead speed of 50 mm/min using a Zwick universal testing machine (Ulm, Germany).

2.5. Dynamic mechanical thermal analysis

The dynamic mechanical properties of the blends were analysed using a dynamic mechanical thermal analyzer (Eplexor 150 N, Gabo Qualimeter, Ahlden, Germany) in tension mode. The static force and dynamic force were taken as 10 and ± 5 N, respectively. Samples of 4 mm thickness and 10 mm width were used. The dynamic frequency was kept constant at 10 Hz and the heating rate was selected as 1 °C/min from -100 to $+100$ °C.

2.6. Dynamic rheology

The rheological properties of the blends were evaluated on a Rheometric Scientific ARES rheometer in plate/plate geometry. Spherical samples of 25 mm diameter and 1 mm thickness were punched out from compression moulded plates and the soak time was carefully adjusted to 3 min. A temperature/-frequency sweep method was selected and the frequency range was taken as 0.1–100 rad/s at three different temperatures 190, 210 and 230 °C. The strain rate was taken as 10%.

3. Results

3.1. Morphology

3.1.1. Uncompatibilised blends

The morphology of cryogenically fractured and extracted surfaces of PA12/PP uncompatibilised blends can be evaluated from Fig. 1. As mentioned earlier, owing to the strong unfavourable interfacial interactions (high-interfacial tension) in the blends, all micrographs exhibit two-phase morphology. More specifically, it can be suggested that all blends except N_{50} and N_{60} possess a typical matrix/droplet morphology of uncompatibilised blends in which the minor component exists as dispersed domains in the matrix of the major component. The morphological parameters estimated from SEM micrographs of uncompatibilised blends with matrix/droplet morphologies are given in Fig. 2(a)–(e).

Fig. 2(a) presents the influence of blend ratio on the average domain size ($\bar{D}_n$ and $\bar{D}_w$) of dispersed particles. It is seen from the figure that, as the weight percent of the dispersed phase increases, particle size increases. It is important to note that for a given dispersed phase concentration (for example, N_{90} and N_{10}) PP domains are smaller than corresponding PA dispersed domains. This is not unexpected and the obvious reason is that the relatively less viscous component (PP) forms smaller dispersed particles in more viscous matrix phase (PA) when all other factors (viz. processing conditions, composition, etc.) are kept constant due to the relatively more restricted diffusion effects imposed by the matrix phase on the coalescence of dispersed particles and the increased shear stress effects resulting from the more viscous matrix phase. This can be evidenced from the complex viscosity values of PA12 and PP presented in Fig. 3. It is seen that PA12 possesses greater viscosity in the whole frequency range. Being more viscous, PA12 imposes greater restricted diffusion effects on

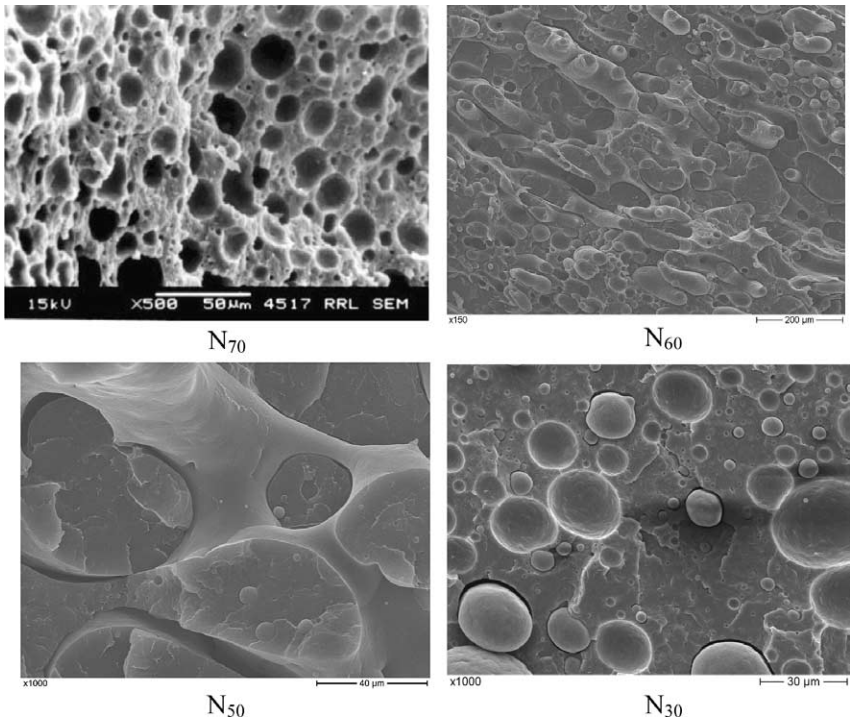

Fig. 1. SEM micrographs of uncompatibilised PA12/PP blends.

the coalescence of PP dispersed particles, which in turn results in smaller PP dispersed domains. On the other hand when PP forms the matrix phase, the coalescence of PA dispersed phase becomes relatively easy due to the lower viscosity of PP.

Fig. 2(b) and (c) demonstrates the effect of blend ratio on the polydispersity index and domain distribution of the dispersed phase, respectively, in PA12/PP uncompatibilised blends. It is quite evident from the figures that PA12/PP uncompatibilised blends possess a broad, non-uniform and unstable morphology. It can also be seen that as the weight percent of the minor component in the blends increases, the non-uniformity increases with simultaneous depletion in the stability. The interfacial area per unit volume (A_i) of dispersed particles presented in Fig. 2(d) implies that blend ratio has no appreciable effect on A_i (except in N_{40} which shows relatively lower value). However, one can see that PP dispersed particles possess relatively higher values. On the other hand, the interparticle distance of dispersed particles (IPD) given in Fig. 2(e) reveals that there is little change in IPD up to 20 wt% of the dispersed phase and, beyond this limit, a decrease in IPD is seen in both PA and PP rich blends. However, interestingly, IPD of N_{40} is slightly greater than that of N_{30}. In short, all morphological parameters display that PA12/PP blends are highly incompatible with a broad, non-uniform and unstable morphology.

3.1.2. Compatibilised blends

The mechanism of the interfacial chemical reactions is based on (a) the amine–anhydride reaction which involves an acid/amide intermediate that cylices to produce an imide group and a water molecule (Fig. 4(a)), or (b) an amide–anhydride mechanism which involves an acid/imide intermediate which cyclices, leading to a cyclic imide and an acid chain end (Fig. 4(b)) [43]. The effect of compatibiliser concentration on the morphology of dispersed phase in N_{70} and N_{30} blends can be evaluated from the SEM micrographs of cryogenically fractured and extracted surfaces of the specimens demonstrated in Figs. 5 and 6, respectively. Fig. 7 presents the effect of compatibiliser concentration on the dispersed particle size in both N_{70} and N_{30} blends. A drastic reduction in particle size with increase in compatibiliser concentration can be seen in both blends. However, one can infer that a more significant drop in particle size is observed in N_{30} blends. It should also be noted that in both blends, after the initial sharp decline in particle size, a quasi-equilibrium state is attained beyond a critical compatibiliser concentration called critical micelle concentration, CMC (5 wt% of compatibiliser in the present case). Attention should be paid to the fact that a leveling off of particle size is achieved at the same compatibiliser concentration in both blends.

Effect of compatibiliser concentration on the distribution of dispersed particles in both N_{70} and N_{30} blends is given in Fig. 8(a)–(c). Domain distribution becomes narrow indicating a more fine, uniform and stable morphology in presence of compatibiliser. However, it is interesting to note that for N_{70} blends, beyond CMC (5 wt%), there is little change in distribution of particles while in N_{30} blends, 10 wt% compatibiliser provides more uniform particle distribution. In Fig. 9, one can see an appreciable increase in A_i of dispersed particles with increase in compatibiliser concentration up to 5 wt% of compatibiliser (CMC). Beyond that limit, an almost

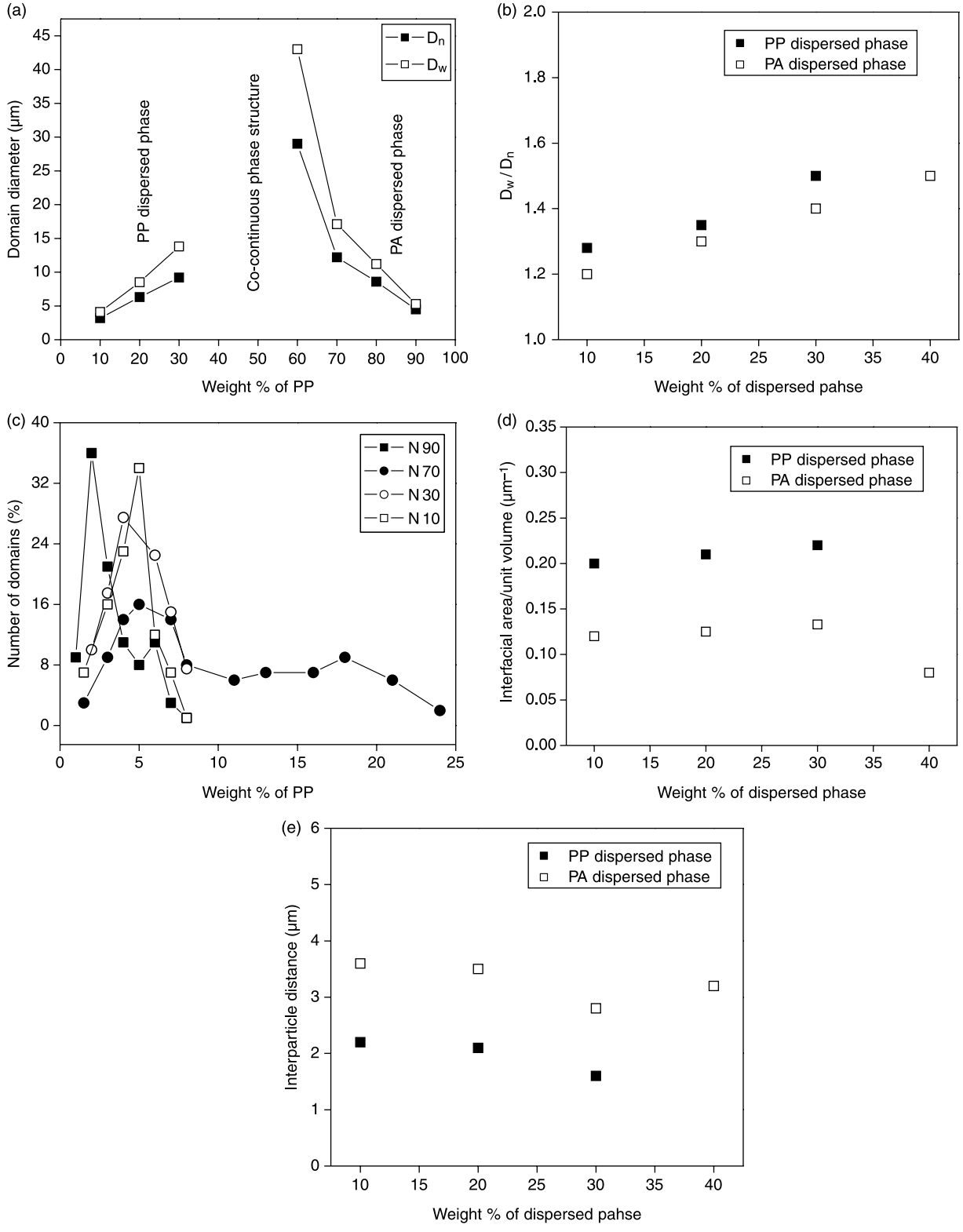

Fig. 2. Effect of blend ratio on the morphological parameters of uncompatibilised PA12/PP blends: (a) average domain size; (b) polydispersity index; (c) domain distribution; (d) interfacial area per unit volume; (e) interparticle distance.

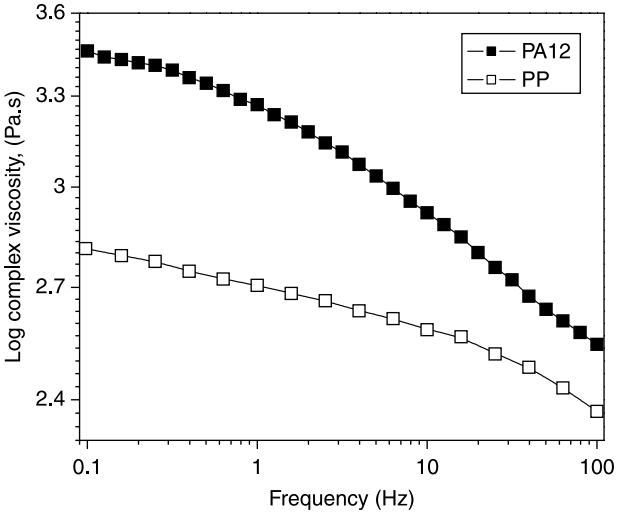

Fig. 3. Variation of complex viscosity of PA12 and PP as a function of frequency.

leveling off in A_i is observed. On the other hand, just reverse trend is seen in the case of interpartice distance (IPD) displayed in Fig. 10. It is seen that IPD of particles decreases with increase in compatibiliser concentration up to CMC and beyond that limit, a leveling off in IPD results.

3.2. Mechanical properties

3.2.1. Uncompatibilised blends

The tensile properties such as ultimate tensile strength (σ_m), elongation at break (ε_b) and Young's modulus (E) of uncompatibilised PA12/PP blends are presented in Table 1. σ_m and ε_b revealed that all the blends possess inferior properties owing to the highly immiscible and incompatible nature. Despite showing negative deviation, one can also find a difference in behaviour in both σ_m and ε_b. Note that σ_m showed minimum properties for blends containing 40–60 wt% of PP (N_{60}, N_{50} and N_{40}), while ε_b of these blends, interestingly, is marginally higher than the blends with 30 wt% of the dispersed phase. On the other hand, E of blends exhibits a different trend. It is seen that E of all blends except N_{60}, N_{50} and N_{40} is almost the same indicating that the blend ratio has no appreciable influence on the E of uncompatibilised blends except for N_{60}, N_{50} and N_{40} blends.

3.2.2. Compatibilised blends

Effect of compatibilisation on the tensile strength of PA12/PP blends is shown in Fig. 11. It can be seen that the presence of compatibiliser tremendously enhanced the tensile strength of all blends. It is noteworthy that the extent of

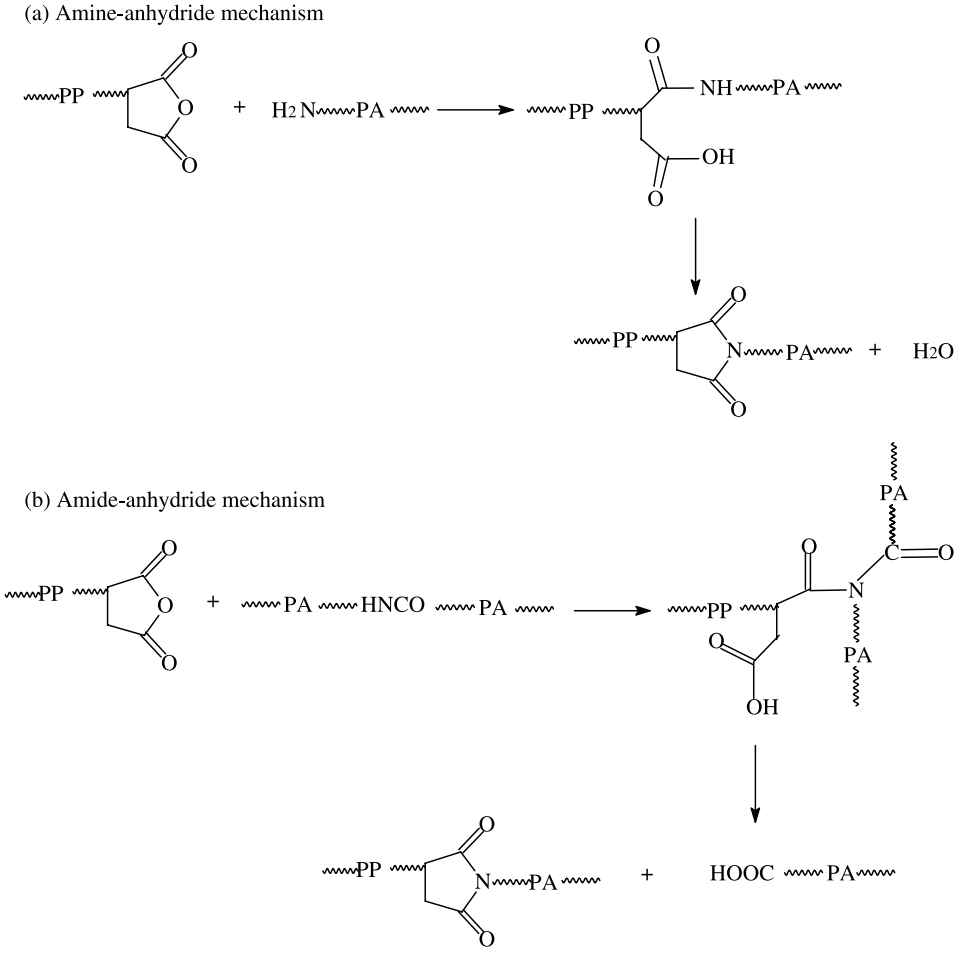

Fig. 4. The mechanism of interfacial chomical reaction between PA12 and PP-*g*-MA (a) Amine–anhydride mechanism, (b) amide–anhydride mechanism.

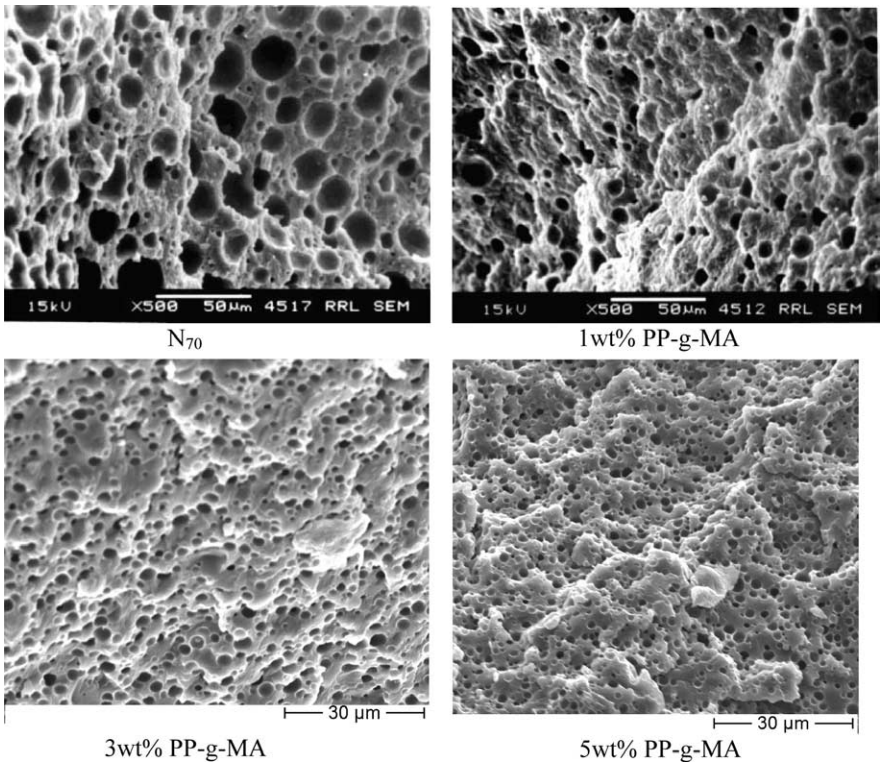

Fig. 5. SEM micrographs of N_{70} blends in presence and absence of compatibiliser.

improvement is maximum in N_{50} (~150%), followed by N_{70} (~85%), while N_{30} registered relatively 'less improvement' (~50%) in tensile strength. Attention should also be paid to the fact that 10 wt% compatibiliser is required to attain maximum strength (except for N_{30} where 5 wt% of compatibiliser was sufficient) beyond which a leveling off in tensile strength is observed. However, the incorporation of compatibiliser up to 5 wt% marginally decreased the ε_b of N_{50} and N_{30} blends

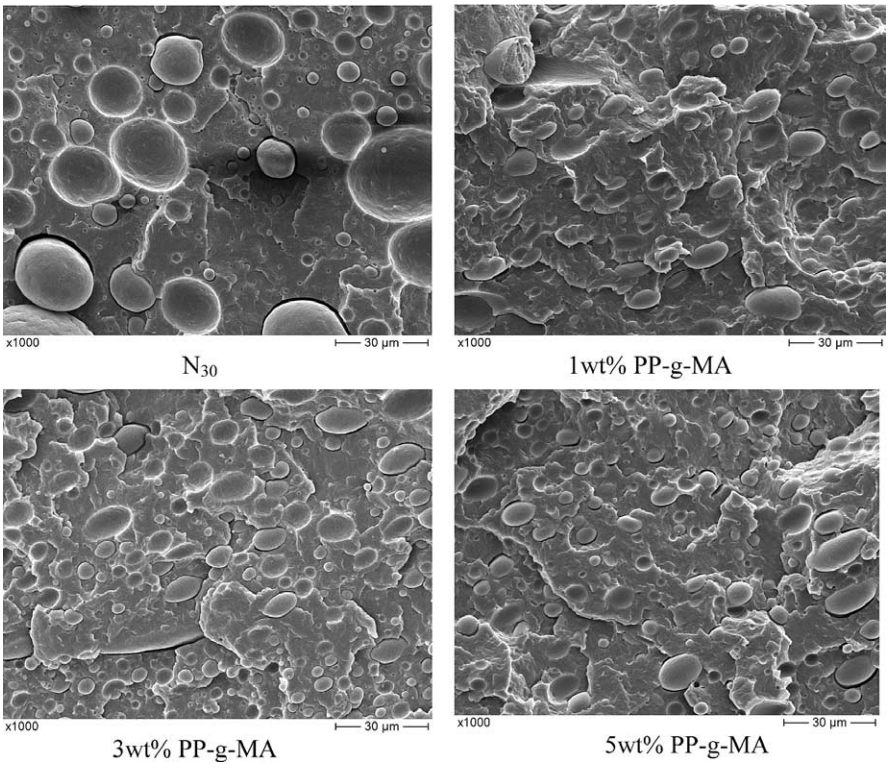

Fig. 6. SEM micrographs of N_{30} blends in presence and absence of compatibiliser.

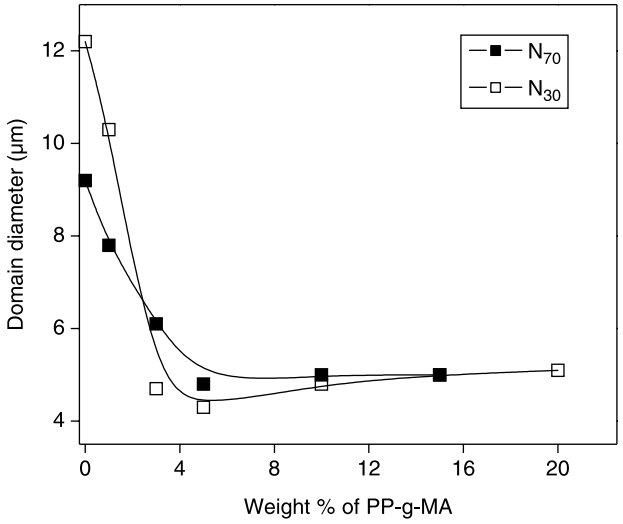

Fig. 7. Effect of PP-*g*-MA on the dispersed particle size of PA12/PP blends.

followed by a leveling off beyond that limit (for N_{30} leveling off is observed beyond 10 wt%), where as a slight increase in ε_b is noted for N_{70} (Table 2). On the other hand, the E values of blends are little affected by the presence of compatibiliser as obvious from Table 2.

4. Discussion

From the morphology of uncompatibilised PA12/PP blends, one can observe two main facts: (a) all blends exhibit a non-uniform and unstable morphology and (b) as the weight percent of the dispersed phase increases, the morphology becomes less stable. This can be better explained in terms of interfacial tension and coalescence effects. It is, as mentioned earlier, unequivocally established that the final morphology is determined by the deformation–disintegration phenomena and coalescence. The relative importance of applied viscous force and counteracting interfacial force can be expressed by Taylor equations (Eqs. (6) and (7)) derived from the studies of deformation and disintegration of the dispersed phase for Newtonian systems in simple shear fields in the absence of coalescence effects [44]. Taylor defined a dimensionless parameter E which is given as Eq. (6).

$$E^* = \mathrm{Ca}\left[\frac{(19p+16)}{(16p+16)}\right] \tag{6}$$

Ca, capillary number, represents the ratio of viscous to surface tensional forces.

$$\mathrm{Ca} = \frac{\eta_m \dot{\gamma} R}{\sigma} \tag{7}$$

where η_m is the viscosity of the matrix, p the viscosity ratio of the droplet phase to the matrix, R the radius of the droplet, $\dot{\gamma}$ the shear rate and σ the interfacial tension. If Ca is small, the interfacial forces dominate and a steady drop shape develops. When Ca exceeds a critical value, Ca_{crit} the droplet will deform and subsequently breaks up under the influence of interfacial tension.

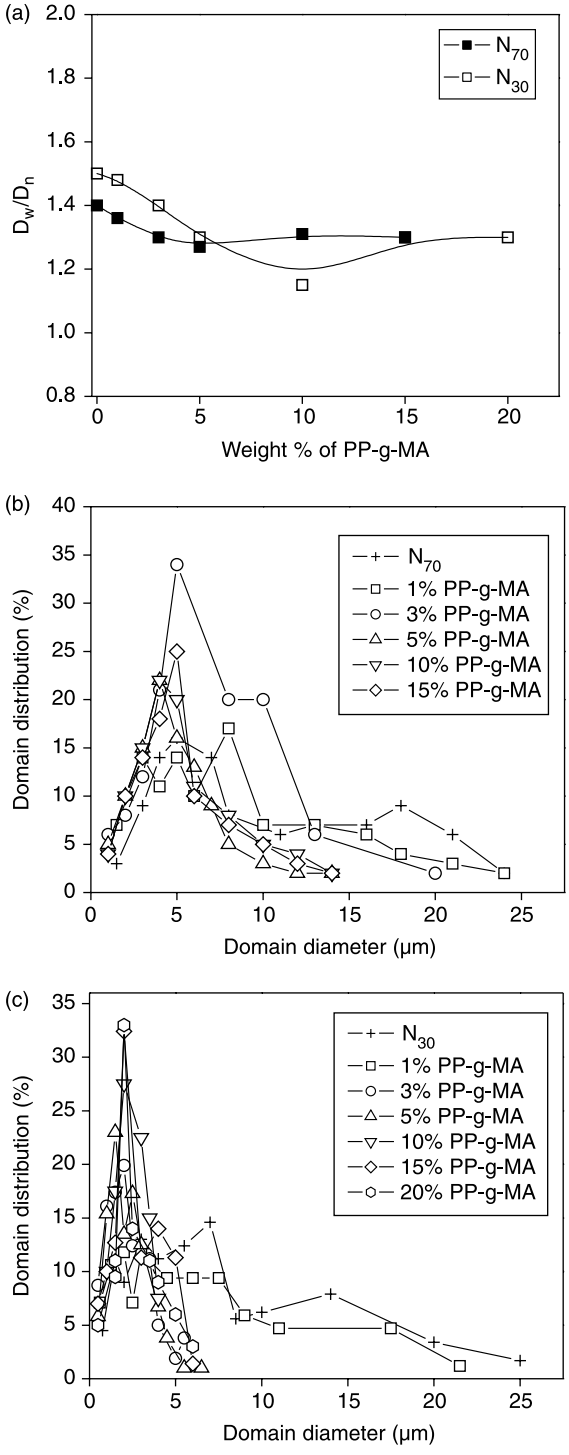

Fig. 8. Effect of PP-*g*-MA on the (a) poly dispersity index of PA12/PP blends; (b) domain size distribution of N_{70} blends; (c) domain size distribution of N_{30} blends.

Taylor also derived an expression for Ca_{crit} in the simple shear flow from a Newtonian flow as:

$$\mathrm{Ca}_{crit} = \frac{1}{2}\left[\frac{(16p+16)}{(19p+16)}\right] \tag{8}$$

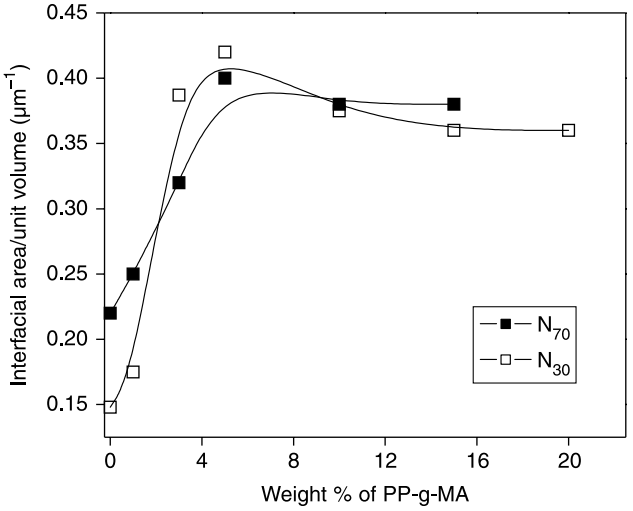

Fig. 9. Effect of PP-*g*-MA on the interfacial area per unit volume of dispersed particles in PA12/PP blends.

Using $Ca = Ca_{crit}$, one can calculate the droplet diameter D as:

$$D = \frac{2Ca_{crit}\sigma}{\dot{\gamma}\eta_m} \quad (9)$$

Later, Wu [42] modified this equation as:

$$D = \frac{4\sigma p^{\pm 0.84}}{\dot{\gamma}\eta_m} \quad (10)$$

The exponent is positive for $p > 1$ and negative for $p < 1$.

Serpe et al. [45] further modified this equation by using the blend viscosity rather than the matrix viscosity and by considering a term of composition (thus coalescence effects), as follows

$$D = \frac{4\sigma(\eta_d/\eta_b)^{\pm 0.84}}{\dot{\gamma}\eta_b[1-(4\phi_d\phi_m)^{0.8}]} \quad (11)$$

Table 1
Effect of blend ratio on the tensile properties of uncompatibilised PA12/PP blends

Blends	Ultimate tensile strength (MPa)	Elongation at break (%)	Young's modulus (MPa)
N_{100}	45.0±1.3	75±3	1550±58
N_{90}	40.3±1.2	43±2	1530±47
N_{80}	31.7±0.7	33±2	1490±35
N_{70}	23.9±0.6	18±2	1540±67
N_{60}	17.7±0.7	24±3	1155±78
N_{50}	15.9±0.8	32±3	1340±67
N_{40}	18.7±0.8	27±2	1170±69
N_{30}	20.7±0.9	20±2	1490±55
N_{20}	25.4±0.7	23±2	1640±62
N_{10}	31.3±0.4	27±3	1540±57
N_0	35.0±0.3	27±2	1660±43

where η_d is the viscosity of the dispersed phase and ϕ_i is the volume fraction of component i.

From Taylor equations (Eqs. (6) and (7)), it is seen that size of dispersed particles is directly related to the interfacial tension between the two phases. At the same time, Favis [46] has shown that blend morphology is not sensitive to 2–3-fold changes in shear stress and shear rate in an internal mixer. Moreover, a direct experimental confirmation of interfacial tension/particle size relationship as predicted by Taylor theory has been demonstrated by Lepers et al. [47] who argued that in the absence of coalescence effects, there is a close 1:1 relationship between morphology and interfacial tension. Liang et al. [48] have investigated on the correlation between the interfacial tension and dispersed phase morphology in interfacially modified blends of linear low density polyethylene (LLDPE) and polyvinyl chloride (PVC) and based on the results, they demonstrated a direct experimental confirmation of the interfacial tension/phase size relationship as predicted by Taylor theory. According to the authors, there is a 1:1 relationship between droplet size and interfacial tension that is independent of the emulsification efficacy of the

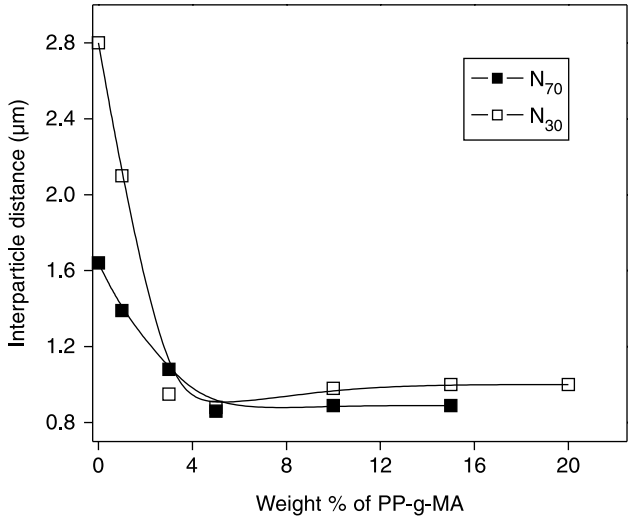

Fig. 10. Effect of PP-*g*-MA on the interparticle distance of dispersed particles in PA12/PP blends.

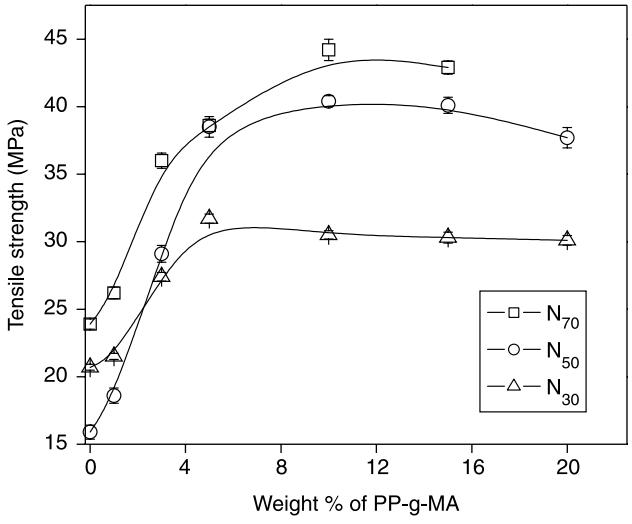

Fig. 11. Effect of compatibiliser concentration on the ultimate tensile strength of PA12/PP blends.

Table 2
Effect of compatibiliser concentration on the elongation at break and Young's modulus of PA12/PP blends

Weight percentage of PP-*g*-MA	Elongation at break (%)			Young's modulus (MPa)		
	N_{70}	N_{50}	N_{30}	N_{70}	N_{50}	N_{30}
0	18±2	32±3	20±2	1540±67	1340±67	1490±55
1	20±1	30±2	18±1	1490±40	1310±30	1520±36
3	22±1	25±1	14±1	1500±40	1360±27	1540±37
5	24±1	21±1	11±1	1520±40	1390±23	1550±28
10	22±1	14±1	10±1	1590±42	1410±18	1570±29
15	20±1	14±1	9±1	1620±36	1430±21	1620±31
20	–	10±1	9±1	–	1420±25	1630±32

compatibiliser. So the high interfacial tension situation due to the unfavourable interactions at the interface between the components in uncompatibilised PA12/PP blends is one of the basic reasons for the existence of a non-uniform unstable morphology.

Further, Tokita [49] derived an expression for the particle size of the dispersed phase in polymer blends that incorporates composition as variable. According to this theory, at equilibrium, when coalescence and break down are balanced, the equilibrium particle size (d_e) is given by

$$d_e \cong \frac{24P_r\sigma}{\pi\tau_{12}}\left\{\phi_d + \left(\frac{4P_rE_{dk}}{\pi\tau_{12}}\right)\phi_d^2\right\} \quad (12)$$

where τ_{12} is the shear stress; σ, the interfacial tension; E_{dk}, the bulk breaking energy; ϕ_d, the volume fraction of the dispersed phase and P_r the probability for a collision to result in coalescence. Tokita's theory predicted that particle size at equilibrium diminishes as the magnitude of the stress field increases while an increase in interfacial tension between the phases and volume fraction of the dispersed phase result in an enhancement of particle size. Thus one can claim that the increase in particle size with increase in concentration of the dispersed phase in PA12/PP blends is mainly due to the increase in coalescence (since interfacial tension between the components—PA12 and PP—remains almost unaffected) which may arise due to any of the following interactions such as:

(i) van der Waals' forces between neighbouring particles;
(ii) random mechanical forces exerted on dispersed particles by irregular motion;
(iii) capillary forces;
(iv) buoyancy resulting from different gravitation of the two components (can be neglected for systems with little difference in density); and
(v) friction resulting from viscous flow.

In short, the broad, non-uniform and unstable morphology of uncompatibilised blends is basically derived from the high interfacial tension and coalescence conditions, and the composition dependence of morphology is a direct result of coalescence.

The main features that can be seen in the morphological investigation of compatibilised blends comprise: (a) stabilisation of morphology in presence of compatibiliser as envisaged from morphological parameters and (b) accomplishment of a quasi equilibrium state in morphological parameters beyond CMC owing to interfacial saturation. The former can be explained by taking into account of both reduction in interfacial tension and coalescence rate as a result of emulsification while the latter is due to the micelle formation of the excess compatibiliser in one of the phases as well as the change in its molecular state at interface. It has been reported that the dominant mechanism for particle size reduction is mainly caused by the suppression of coalescence [50,51]. The compatibiliser has been proposed to act as a steric stabiliser, due to compression of part of the compatibiliser extending into the matrix [5,25]. At the same time, a different mechanism has been emerged from a number of studies which suggest that the bulk flow convects the compatibiliser away from the film region and the stress results from the resulting gradient in interfacial tension (Marangoni stress) retards the drainage of the film between the droplets [52,53]. Anastasiadis et al. [54] have observed a sharp decrease in interfacial tension with the addition of small amount of block copolymer followed by a levelling off as the copolymer concentration is increased above the apparent CMC.

One can also note a close correlation between the morphology and tensile properties of PA12/PP uncompatibilised blends. In fact, the inferior tensile properties of the blends directly result from the unstable and non-uniform morphology as indicated by the morphological parameters of the uncompatibilised blends. Further, as the amount of dispersed phase increases, 'morphological stability' decreases and consequently, deterioration in properties results. Based on these factors, one can claim that, for uncompatibilised blends, blends with co-continuous phase structure appeared to possess least stable morphology (owing to the maximum unfavourable interaction) and thereby exhibit maximum deterioration in tensile strength. However, the elongation at break values of the blends offer an apparent conflict with the aforementioned fact.

Further evidence in this direction can be drawn from the dynamic mechanical properties of the uncompatibilised blends demonstrated in Fig. 12(a)–(c). The temperature dependence of loss modulus and tan δ presented in Fig. 12(b)–(c) clearly reveals that there are no favourable interactions between PA12 and PP, as their transition peaks (T_g of PA12 ~55 °C, T_g of PP ~2 °C and β-transition of PA12 ~ −58 °C) experience no

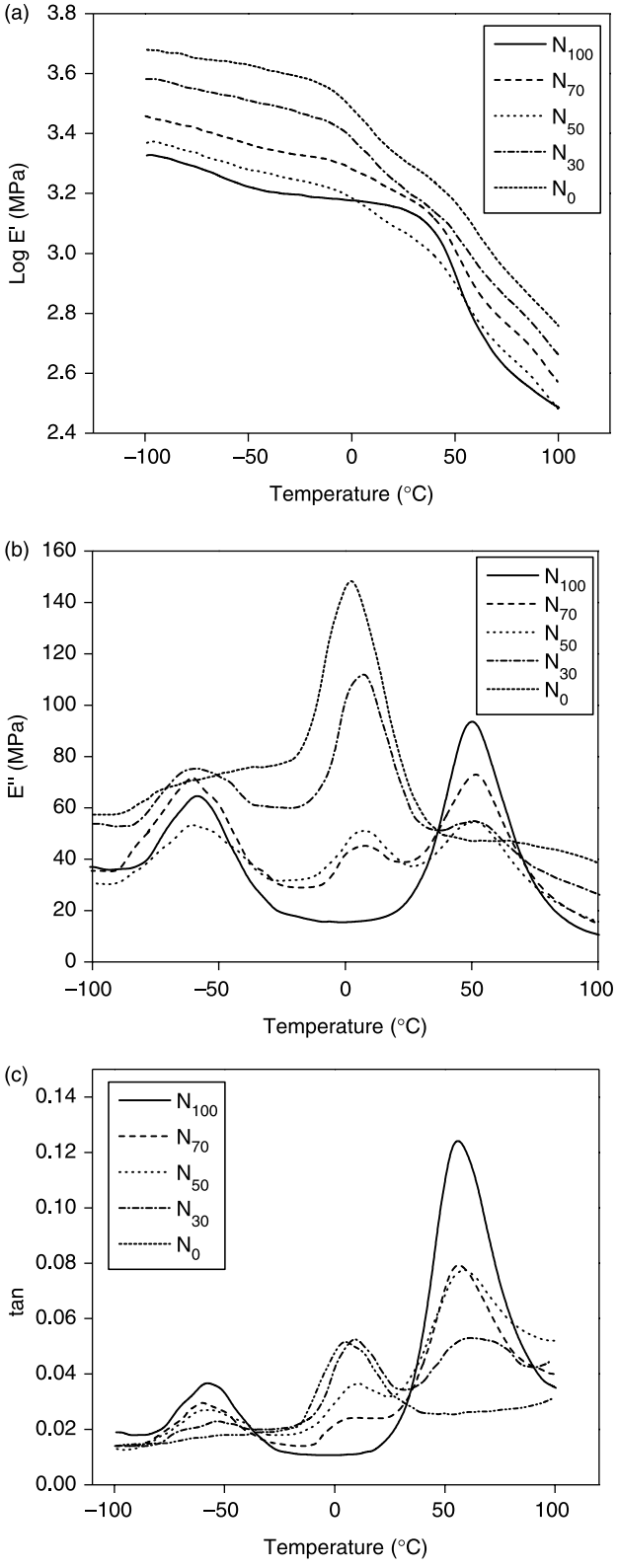

Fig. 12. (a) Dependence of storage modulus on temperature in PA12, PP and their blends; (b) dependence of loss modulus on temperature in PA12, PP and their blends; and (c) dependence of tan δ values on temperature in PA12, PP and their blends.

Table 3
Storage modulus of PA12, PP and their blends at room temperature

Blend	E' (MPa)
N_{100}	1410
N_{70}	1550
N_{50}	1200
N_{30}	1640
N_0	2050

shift as a function of blend ratio. It is also important to note that the Young's modulus (E) of the blends offer no change on blending, in contrary to other tensile properties. However, this is not unexpected since E, which is estimated at very low strain level does not depend appreciably on the incompatibility factor as other tensile properties. Despite this factor, it is seen that E of N_{40}, N_{50} and N_{60} registered lower values. Note that both N_{50} and N_{60} blends exhibit co-continuous phase structure and one can thus claim that there is a link between the morphology and Young's modulus at 'strong' incompatibility level. At the same time, one can see a similar observation in Fig. 12(a) which shows the dependence of storage modulus (E') of uncompatibilised blends as a function of temperature. It is seen that E' of N_{50} is less than that of all the blends in the whole temperature range. Attention should also be paid to the fact that at around room temperature (RT) E' of N_{50} becomes exceptionally low and found to be even lower than that of PA12 (Interestingly, it is the glass transition region of PP). But beyond 40 °C, the E' of N_{50} crosses over that of PA12. The values of E' at RT for all the blends are given in Table 3. Also note that the E' of PP and PP rich blends experiences similar decrease in this region. So, it can be assumed that the lower values of Young's modulus for N_{40}, N_{50} and N_{60} arise due to the combined effects of the glass transition of PP (that acts as continuous phase) and the relatively lower modulus of PA12 in addition to the strong incompatibility.

5. Comparison of the experimental compatibilisation data with theory

The basic factors which influence the interfacial properties were estimated by Leibler [55] in terms of scaling arguments. Noolandi and co-workers [56,57] developed mean field theories of polymer interfaces. Leibler's theory is valid for nearly miscible systems where as mean field theories are applicable to highly immiscible systems. According to Noolandi [57], the effect of copolymer on surface tension between the two phases is mainly influenced by the contributions from a series of factors such as lowering of interaction energy between the immiscible homopolymers, the broadening of the interface between the homopolymers, the entropy reduction in the system, decrease in energy of interaction of the two blocks with each other and a large decrease in the interaction energy of the oriented blocks with homopolymers. However, it should be noted that the localisation of copolymer at the interface and the separation of blocks into corresponding homopolymer phases and the simultaneous reduction in interfacial tension between

the phases depend on various factors such as mixing conditions, interaction of the compatibiliser with the dispersed phase, molecular weight and composition of the compatibiliser, the rate of absorption and orientation of the compatibiliser at the interface. Based on these facts and by neglecting the loss of conformational entropy, Noolandi derived an equation for the interfacial tension reduction as

$$\Delta\Gamma = d\phi_c\left[1/2\chi + 1/Z_c - 1/Z_c \exp(Z_c\chi/2)\right] \quad (13)$$

where d is the width at half height of the copolymer profile reduced by the Kuhn statistical segment length, $\phi_c$the bulk copolymer volume fraction of the copolymer in the system, Z_c the degree of polymerisation of the copolymer and χ the Flory–Huggins interaction parameter between A and B segments. Although the theory was developed for the action of a symmetrical di block copolymer, A-*b*-B, it can be applicable to other systems too where the compatibilising action is not strictly by the addition of block copolymers. As the interfacial tension reduction is directly proportional to the particle size reduction (ΔD) [42], it can be argued that

$$\Delta D = Kd\phi_c[1/2\chi + 1/Z_c \exp(Z_c\chi/2)] \quad (14)$$

where K is a proportionality constant. Fig. 13(a) represents the percent reduction in particle size as a function of compatibiliser concentration in N_{70} blends. It can be seen that below a CMC, the drop in ΔD is almost linear, where as beyond CMC, a levelling off is observed. This is in agreement with the predictions of Noolandi and Hong [56]. A similar trend can be assessed from Fig. 13(b), which gives the variation in ΔD as a function of compatibiliser concentration in N_{30} blend. One can evaluate both the efficiency of compatibilisers as well as the optimum amount of compatibiliser required to saturate the interface.

The interfacial area per unit volume occupied by each compatibiliser molecule is given by the expression [58]

$$\Sigma = \left(\frac{3\phi M}{RNW}\right) \quad (15)$$

where N is Avogadro number, M the number average molecular weight of the compatibiliser, R the average radius of the dispersed phase, ϕ the volume fraction of the dispersed phase and W the weight of the compatibiliser required per unit volume of the blend. When ϕ and M are kept constant, Σ depends on the values of R and W. R decreases with increase in the weight fraction of the compatibiliser and Σ may either decrease or not change or increase. Hosoda et al. [59] have reported that the product of RW remained constant and did not change with W for PP-*g*-MA/PA 30/70 blend. On the other hand, Tang and Huang [60] found a decrease in Σ with an increase in compatibiliser concentration in four blends, viz. PA/PP = 90/10, 10/90 and PA/PE = 90/10, 10/90. The effect of compatibiliser concentration in PA12/PP blends on Σ can be evaluated from Fig. 14. We observed a decrease in Σ with increase in concentration of the compatibiliser. This does not mean that as the amount of compatibiliser in the blend increases, the tendency to form micelles increases. A plausible

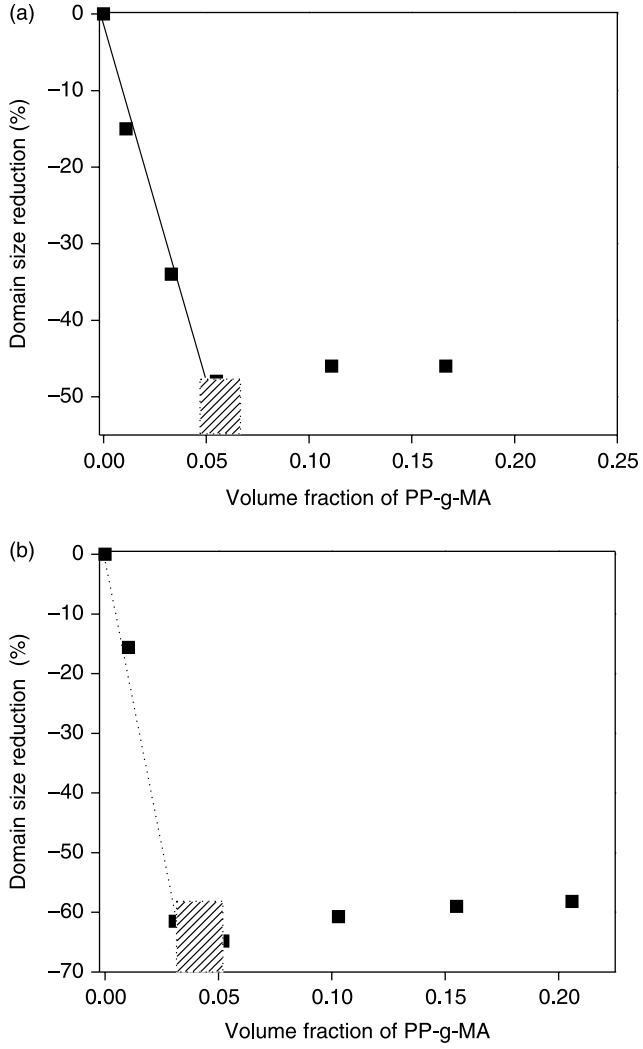

Fig. 13. Effect of PP-*g*-MA on the domain size reduction of (a) N_{70} blends; (b) N_{30} blends.

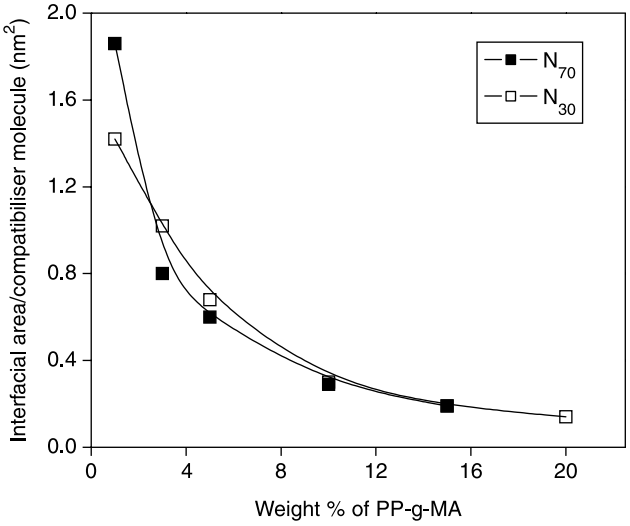

Fig. 14. Effect of PP-*g*-MA on the interfacial area per unit volume of the compatibiliser molecule of PA12/PP blends.

explanation is that when the concentration of compatibiliser is less, each molecule occupies more interfacial area than when the compatibiliser concentration is high, where the compatibiliser molecules are forced to arrange themselves at the interface so as to occupy smaller interfacial area per compatibiliser molecule. Thus, one can conclude from the above facts that the molecular state of compatibillizer changes with the concentration of the compatibiliser in the blend.

Leibler [55] examined the emulsifying effect of an A–B copolymer in an immiscible blend of polymers A and B and predicted a reduction of interfacial tension caused by equilibrium adsorption of the copolymer at the interface. He suggested that at equilibrium, the droplet size distribution is controlled by rigidity and spontaneous curvature of radius of the interphase, both dependent on the copolymer's molecular constitution. According to the author, the interfacial tension reduction is given by the relation

$$\Delta\Gamma = -(kT/a^2)(3/4)^{1/3}(\Sigma/a^2)^{-5/3}(Z_{CA}Z_A^{-2/3} + Z_{CB}Z_B^{-2/3}) \quad (16)$$

where Z_{CA} and Z_{CB} are the number of A and B units in the copolymer, respectively, Z_A and Z_B the degree of polymerisation of A and B, respectively, a the monomer's unit length, Σ the interfacial area per copolymer. In Leibler's theory, a block copolymer was used as a compatibilizer. Between the two brush limits in Leibler's theory [55], prediction based on dry brush limit in which the homopolymer does not penetrate the brush formed by the copolymer, has been used. Based on the assumption that the reaction between reactive compatibilizer and the polymer with a different functional group occurs near the interface, one can use the following equation for the interfacial tension reduction ($\Delta\Gamma$) obtained by the brush limit which is independent of the homopolymer molecular weights [19].

$$\frac{\Delta\Gamma}{\Gamma_0} = \left(\frac{\sqrt{48}}{9}\right)\mu^{3/2}(\chi N)^{-1/2} \quad (17)$$

where Γ_0 is the interfacial tension of polymer blend without a compatibiliser and μ is the chemical potential which is given by the equation

$$\mu = \ln\phi^+ + f\chi N \quad (18)$$

where f is the volume fraction of the component in copolymer which is miscible to homopolymer forming the dispersed phase and

$$\phi^+ = \frac{\phi_0}{[\phi_m + \phi_d \exp\{\chi(N_A - N_B)\}]} \quad (19)$$

where ϕ_0, ϕ_m and ϕ_d represent the volume fraction of the copolymer, matrix and dispersed phase, respectively, N_A and N_B are the number of segments of the component in the copolymer miscible to the homopolymer forming the dispersed phase and that miscible to homopolymer forming the matrix phase, respectively. Since the value of $\exp\{\chi(N_A - N_B)\}$ is negligible compared to ϕ_m, ϕ^+ is expressed by ϕ_0/ϕ_m.

The surface coverage of one copolymer, i.e. the surface area occupied by one compatibiliser molecule per unit volume at the interface, is related to μ and χ as

$$\left[\frac{\Sigma}{b^2}\right] = (3/2)(N/\mu)^{1/2} \quad (20)$$

where b is the kuhn length, which refers to the effective monomer size for the equivalent freely jointed chain.

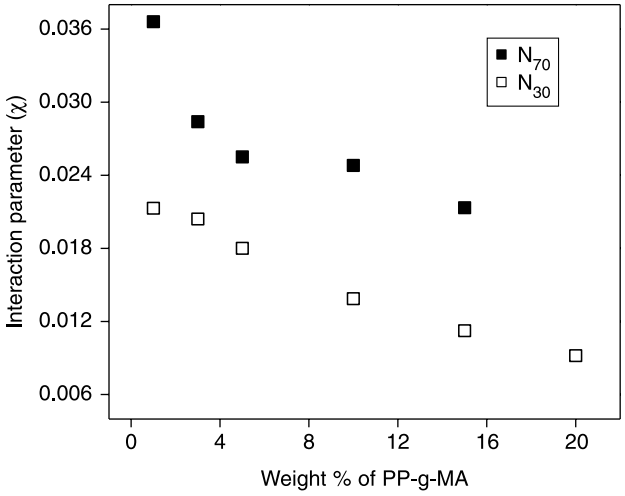

Fig. 15. Effect of PP-*g*-MA on the χ values calculated by the dry brush limit of Leibler's theory.

Since the dispersed particle reduction is directly proportional to the interfacial tension reduction, the following equation can be used:

$$\frac{\Delta\Gamma}{\Gamma_0} = \frac{(\Gamma_0 - \Gamma)}{\Gamma_0} \approx \frac{\Delta D}{D} = \frac{(D_0 - D)}{D_0} \quad (21)$$

The variation in values of χ as a function of PP-*g*-MA in N_{70} and N_{30} blends is given in Fig. 15. It is seen from the figure that N_{30} blends exhibited lower χ values in presence of compatibiliser. As the amount of PP-*g*-MA increases, χ values diminish indicating enhanced interaction between the phases at interface in presence of compatibiliser. However, note that the theoretically calculated χ values from Leibler's theory show apparent conflict with the experimental observation, which shows a decrease in particle size followed by a quasi-equilibrium state beyond CMC owing to interfacial saturation. For χ values there exists no true levelling off beyond CMC of the compatibiliser, especially for N_{30} blends. It is also interesting to note that the χ values calculated using Leibler's theory in presence of compatibiliser are appreciably less than χ value (0.365) obtained for PA12/PP uncompatibilised blends theoretically calculated (from molar attraction constants from Hoy's scale) using Hildebrand–Scatchard–van Laar equation

$$\chi_{12} = \frac{V_r}{RT}(\delta_1 - \delta_2)^2 \quad (22)$$

where V_r is the reference volume, δ_1 ($=9.69$ $(cal/cm^3)^{1/2}$) and δ_2 ($=7.82$ $(cal/cm^3)^{1/2}$) the solubility parameters of PA12 and PP, respectively, and T is the temperature in absolute scale.

The big difference between the two may be due to the fact that: (i) Leibler's theory was originally proposed for nearly compatible blends and (ii) Liebler's theory is formulated

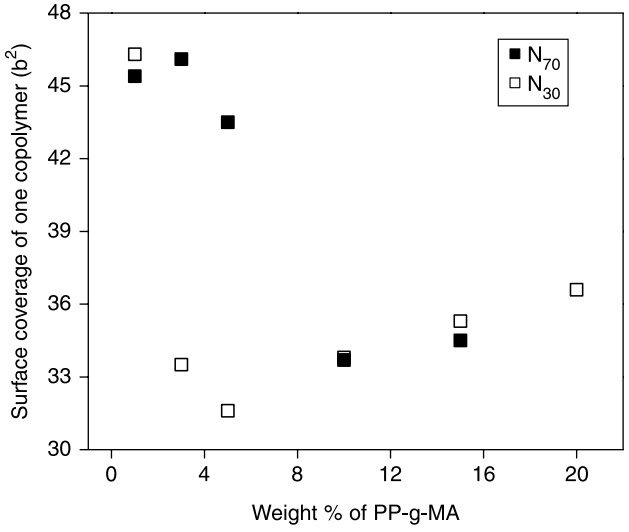

Fig. 16. Effect of PP-*g*-MA on the Σ/b^2 values calculated by the dry brush limit of Leibler's theory.

basically for block copolymers (note that the reaction between PA12 and PP usually leads to graft copolymers).

The effect of PP-*g*-MA on the calculated values of surface coverage of one copolymer presented in Fig. 16 shows that the surface coverage (interfacial area occupied by one copolymer molecule per unit volume, Σ), in general, decreases with increase in PP-*g*-MA up to a certain compatibiliser concentration (5 and 10 wt% for N_{30} and N_{70} blends, respectively) and beyond that limit a slight increase is noted. The decrease in surface coverage indicates that smaller surface area is needed for a copolymer molecule as the concentration of PP-*g*-MA increases and exhibits a similar behaviour to that calculated from equation (15) given by Paul and Newman [58]. This is fundamentally because of the fact that as the χ value decreases, as mentioned earlier, less stretching of graft copolymer chain is needed near the interface and the molecular state of the compatibiliser changes. However, one can note apparent conflict between the calculated values of Σ using Eqs. (15) and (20). (i) When Eq. (15) is used a gradual decrease in Σ is observed with increase in PP-*g*-MA concentration for the whole range of compatibiliser composition whereas an increase was noted beyond a certain level of compatibiliser concentration (5 wt% for N_{30} and 10 wt% for N_{70} blends) when Eq. (20) is used, (ii) The values obtained from Eq. (15) are considerably smaller than those from Eq. (20) which can be explained if one considers the fact that Σ calculated using Eq. (15) is based on the assumption that all the compatibiliser molecules go to the interface.

Based on the fact that upon the addition of compatibiliser, interfacial tension σ decreases and on assumption that the decrease is directly proportional to the interfacial tension difference at a particular compatibiliser concentration C and CMC, then

$$-\left(\frac{d\sigma}{dC}\right) = K(\sigma - \sigma_s) \tag{23}$$

Table 4
Effect of compatibiliser concentration on the rate constant for the change in interfacial tension (K) in N_{70} and N_{30} blends

Weight percentage of PP-*g*-MA	K value	
	N_{70}	N_{30}
1	0.39	0.28
3	0.40	1.04
5	0.94	1.01
10	0.29	0.29
15	0.19	0.17
20	0.13	0.12

where K is the rate constant for the change in interfacial tension with concentration of the compatibiliser, σ the interfacial tension at a given compatibiliser concentration, C and σ_s the interfacial tension at CMC. From the above expression, Tang and Huang [60] eventually derived the following equation

$$R - R_s = (R_0 - R_s)e^{-KC} \tag{24}$$

where R_0, R and R_s are the average radius of dispersed particles with out compatibiliser, at a given compatibiliser concentration and compatibiliser concentration at CMC, respectively. A plot of $\ln(R - R_s)$ versus C can be used to obtain K from the slope.

Aravind et al. [61] have shown that K value reaches a maximum at CMC and beyond that limit a decrease in K value is observed. The K value obtained as a function of compatibiliser concentration for PA12/PP blends are depicted in Table 4. It is obvious from the table that K value increases with increase in compatibiliser concentration, reaches a maximum at CMC and decreases beyond that limit. It is also seen from the table that the rate constant for the reduction in interfacial tension upon compatibiliser incorporation is appreciable up to CMC. Note that both N_{70} and N_{30} blends possess almost same K values beyond CMC.

6. Conclusions

The present investigation was devoted to evaluate the morphology and mechanical properties of PA12/PP blends in presence and absence of reactive compatibiliser. The morphological parameters and mechanical properties of uncompatibilised blends revealed that these blends are highly incompatible with a two-phase non-uniform unstable morphology due to high interfacial tension and coalescence effects. As the concentration of the dispersed phase increased, the incompatibility enhanced.

Compatibilisation of the blends immensely improved the morphology of the blends by drastically reducing the average particle size as well as inter particle distance and increasing the interfacial area per unit volume. The optimum compatibiliser concentration was observed at critical micelle concentration (CMC) up to which a linear drop in particle size was seen as predicted by the theories of Noolandi and Hong, and beyond which a levelling off in morphological parameters has been noted owing to interfacial saturation. The improvement in morphology in presence of compatibiliser led to an

enhancement in tensile strength in all blends and it was found that the mechanical properties in presence and absence of compatibilisation could be correlated with the morphological parameters of the blends. The experimental compatibilisation data have been compared with the theoretical predictions given by Noolandi and Hong, Paul and Newman, Leibler and Tang and Huang and observed a reasonably good agreement between experiment and theory.

Acknowledgement

The authors are thankful to DST/DAAD exchange research programme. One of the authors, S. Jose is thankful to the University Grants Commission (UGC), New Delhi for the financial support. Thanks are also due to IVW, University of Kaiserslautern, for analytical support.

References

[1] Koning C, van Duin M, Pagnoulle C, Jérôme R. Prog Polym Sci 1998;23:707.
[2] Majumdar B, Paul DR. In: Paul DR, Bucknall CB, editors. Polymer blends: formulation and performance, vol. 1. New York: Wiley; 2000 [chapter 17].
[3] Groeninckx G, Harrats C, Thomas S. In: Baker WE, Scott C, Hua GH, editors. Reactive polymer blending. Munich: Hanser Publishers; 2001 [chapter 3].
[4] Thomas S, Prud'homme RE. Polymer 1992;33:4260.
[5] Macosko CW, Guēgan P, Khandpür AK, Nakayama A, Marechal P, Inoue T. Macromolecules 1996;29:5590.
[6] (a) Lee MS, Lodge TP, Macosko CW. J Polym Sci, Part B: Polym Phys 1997;35:2835.
(b) Lee MS, Lodge TP, Macosko CW. Macromol Chem Phys 1998;199:1555.
[7] Lyu S, Jones TD, Bates FS, Macosko CW. Macromolecules 2002;35:7845.
[8] Hlavatá D, Hromádková J, Fortelný I, Haová V, Pulda J. J Appl Polym Sci 2004;92:2431.
[9] Harrats C, Jérôme R. J Polym Sci, Part B: Polym Phys 2005;43:837.
[10] Tao Y, Lebovitz AH, Torkelson JM. Polymer 2005;46:4753.
[11] Hlavatá D, Horák Z, Hromādkova J, Lednický F, Pleska A. J Polym Sci, Part B: Polym Phys 1999;37:1647.
[12] Harrats C, Fayt R, Jérôme R. Polymer 2002;43:863.
[13] Harrats C, Fayt R, Jérôme R, Blacher S. J Polym Sci, Part B: Polym Phys 2003;41:202.
[14] Harrats C, Dedecker K, Groeninckx G, Jérôme R. Macromol Symp 2003;198:183.
[15] Šmit I, Radonjič G, Hlavatá D. Eur Polym J 2004;40:1433.
[16] Kim J, Gray MK, Zhou H, Nguyen ST, Torkelson JM. Macromolecules 2005;38:1037.
[17] George S, Neelakantan NR, Varughese KT, Thomas S. J Polym Sci, Part B: Polym Phy 1997;35:2309.
[18] Kudva RA, Keskkula H, Paul DR. Polymer 2000;41:225.
[19] Kim JK, Kim S, Park CE. Polymer 1997;38:2155.
[20] Dedecker K, Groeninclx G. Polymer 1998;39:4993.
[21] Thomas S, Groeninckx G. Polymer 1999;40:5799.
[22] Kitayama NK, Keskkula H, Paul DR. Polymer 2000;41:8041.
[23] Rol RT, Groeninckx G, Vinckier I, Moldenaers P, Mewis J. Polymer 2004;45:2587.
[24] Zhang J, Lodge TP, Macosko CW. Macromolecules 2005;38:6586.
[25] Sundararaj U, Macoscko CW. Macromolecules 1995;28:2647.
[26] Lepers JC, Favis BD, Taber RJ. J Polym Sci, Part B: Polym Phys 1997;35:2271.
[27] Lyu SP, Cernohous JJ, Bates FS, Macoscko CW. Macromolecules 1999;32:106.
[28] Dedecker K, Groeninckx G. Polymer 1998;39:4985.
[29] Kim S, Kim JK, Park CE. Polymer 1997;38:1809.
[30] (a) Kudva RA, Keskkula H, Paul DR. Polymer 1998;39:2447.
(b) Kudva RA, Keskkula H, Paul DR. Polymer 1999;40:6003.
(c) Kudva RA, Keskkula H, Paul DR. Polymer 2000;41:239.
[31] Dedecker K, Groeninckx G, Inoue T. Polymer 1998;39:5001.
[32] Dedecker K, Groeninckx G. J Appl Polym Sci 1999;73:889.
[33] Kim JK, Yi DK, Jeon HK, Park CE. Polymer 1999;40:2737.
[34] Martin P, Devaux J, Legras R, van Grup M, van Duin M. Polymer 2001;42:2463.
[35] Majumdar B, Paul DR, Oshinski AJ. Polymer 1997;38:1787.
[36] Dedecker K, Groeninckx G. Macromolecules 1999;32:2472.
[37] Kitayama NK, Keskkula H, Paul DR. Polymer 2000;41:8053.
[38] Pan L, Chiba T, Inoue T. Polymer 2001;42:8825.
[39] Jeon HK, Feist BJ, Koh SB, Chang K, Macosko CW, Dion RP. Polymer 2004;45:197.
[40] Laurens C, Creton C, Léger L. Macromolecules 2004;37:6814.
[41] Kho DH, Chae SH, Jeong U, Kim HY, Kim JK. Macromolecules 2005;38:3820.
[42] (a) Wu S. Polymer 1985;26:1855.
(b) Wu S. Polym Eng Sci 1987;27:342.
[43] Roover BD, Devaux J, Legras R. J Polym Sci, Part A: Polym Chem 1997;35:901.
[44] (a) Taylor GT. Proc R Soc London 1932;A138:41.
(b) Taylor GT. Proc R Soc London 1934;A146:501.
[45] Serpe G, Jarrin J, Dawans F. Polym Eng Sci 1990;30:553.
[46] (a) Favis BD. J Appl Polym Sci 1990;39:285.
(b) Favis BD. Makromol Chem Macromol Symp 1992;56:143.
[47] Lepers JC, Favis BD, Tabar RJ. J Polym Sci B: Polym Phys 1997;35:2271.
[48] Liang H, Favis BD, Yu YS, Eisenberg A. Macromolecules 1999;32:1637.
[49] Tokita N. Rubber Chem Technol 1977;50:292.
[50] Shaughnessy BO, Sawhney U. Macromolecules 1996;29:7230.
[51] Fredrickson GF, Milner ST. Macromolecules 1996;29:7386.
[52] Milner ST, Xi H. J Rheol 1996;40:663.
[53] Cristini V, Blawzdziewicz J, Loewenberg M. J Fluid Mech 1998;366:259.
[54] Anastasiadis SH, Gancarz I, Koberstein JT. Macromolecules; 1989;22:1449.
[55] (a) Leibler L. Makromol Chem Macromol Symp 1988;16:1.
(b) Leibler L. Physica A 1991;172:258.
[56] (a) Noolandi J, Hong KM. Macromolecules 1982;15:482.
(b) Noolandi J, Hong KM. Macromolecules 1984;17:1531.
[57] Noolandi J. Polym Eng Sci 1984;24:74.
[58] Paul DR, Newman S, editors. Polymer blends. New York: Academic Press; 1978.
[59] Hosoda S, Kojima K, Kanda Y, Aoyagt M. Polym Network Blends 1991;1:51.
[60] Tang T, Huang B. Polymer 1994;35:281.
[61] Aravind I, Albert P, Ranganathaiah P, Kurian JV, Thomas S. Polymer 2004;45:4925.